

Enhanced Ordering of Water at Hydrophobic Surfaces

Simona Strazdaite,¹ Jan Versluis,¹ Ellen H. G. Backus,^{1, a)} and Huib J. Bakker¹

FOM Institute AMOLF, Science Park 104, 1098 XG Amsterdam,

The Netherlands

(Dated: 6 November 2013)

We study the properties of water molecules adjacent to a hydrophobic molecular layer with vibrational sum-frequency generation (VSFG) spectroscopy. We find that the water molecules at water/hexane, water/heptane and water/polydimethylsiloxane interfaces show an enhanced ordering and stronger hydrogen-bond interactions than the water molecules at an water/air interface. With increasing temperature (up to 80°C) the water structure becomes significantly less ordered and the hydrogen bonds become weaker.

PACS numbers: 78.47.N-

^{a)}Current address: Max Planck Institute for Polymer Research, Ackermannweg 10, Mainz, Germany.

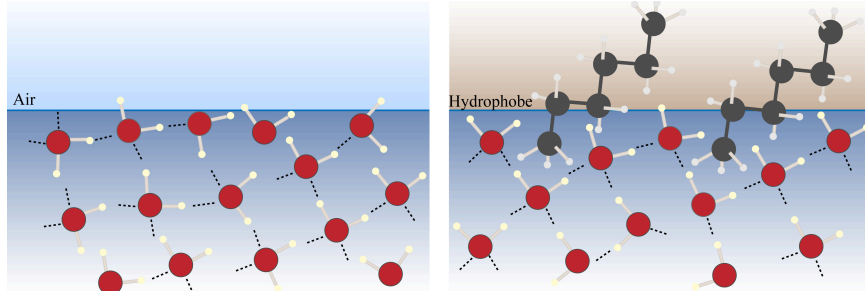


FIG. 1. Schematic representation of water/air (left) and water/hydrophobe (right) interfaces.

I. INTRODUCTION

The interaction between water and hydrophobic molecular groups is of paramount importance in biological processes. For example, hydrophobic hydration is the driving force for protein folding and for lipids to self-assemble into bilipid membranes¹. All these processes are intimately related to the structure and dynamics of the water molecules that solvate the hydrophobic molecular groups. Frank and Evans were the first who investigated the properties of water surrounding hydrophobic molecular groups⁸. They observed that the dissolution of hydrophobes in water is associated with surprising thermodynamic changes like a decrease in entropy and an increase in heat capacity. To explain these observations they proposed the so-called 'iceberg' model for hydrophobic hydration, which implies that water hydrating a hydrophobic solute becomes highly ordered and acquires a structure that resembles that of ice. The iceberg model was later disputed by neutron scattering studies that showed that the water structure near hydrophobic solutes is characterized by an oxygen-oxygen correlation function $g_{OO}(R)$ that is much more similar to that of bulk water than to that of ice^{7,22}.

Recently, a Raman spectroscopy study of the vibrational spectrum of water molecules solvating small alcohols provided the first molecular-scale evidence for the enhanced ordering of water around small hydrophobic solutes⁶. Further evidence for the different behaviour of water molecules in hydrophobic hydration shells was obtained from dynamic studies. Water molecules hydrating hydrophobic molecular groups were observed to show much slower orientational dynamics and hydrogen-bond dynamics than bulk water^{3,9,14,31}. The slowing down of the dynamics of water molecules surrounding hydrophobic groups was reproduced by both classical and *ab initio* molecular dynamics simulations^{27,33}.

An ideal technique to measure the structure of water at water/hydrophobe interface is vibrational sum-frequency generation (VSFG). In VSFG a tunable infrared light beam and a visible light beam are combined to generate light at their sum frequency. The generation is enhanced if the infrared light is resonant with a molecular vibration. VSFG is a surface sensitive technique. The interface specificity arises from the fact that within the dipole approximation VSFG can occur only in media that lack inversion symmetry. Most bulk materials are oriented randomly, meaning that they have an inversion symmetry, but at the interface the symmetry is broken. Hence VSFG allows the selective probing of the layer of water molecules that are in direct contact with hydrophobic material. The SFG spectrum provides detailed information about vibrations and relative orientations of molecules at the interface. This technique has been extensively used to study the structure and hydrogen bonding of water in different systems: salt solutions^{12,16,25,29}, charged interfaces^{13,21}, lipid monolayers^{2,32}.

Only few SFG studies of water/oil systems have been reported, probably because it is not straightforward to produce a stable water/oil interface. The Shen group has measured the structure of water at a fused quartz surface covered with an octadecyltrichlorosilane (OTS) monolayer²⁶. The SFG spectrum was observed to be red shifted compared to that of a water/air interface, which was attributed to the adsorption of hydroxide ions to the interface of the hydrophobic tails of OTS and water. However, in another study of the same Quartz/OTS/water system, the changes in the SFG spectra were attributed to the water molecules that are adsorbed near the polar head groups of the OTS molecules and the quartz surface. Roke and coworkers studied water/oil interfaces with SFG scattering experiments on oil droplets dispersed in water²⁸. From the interference of the low-frequency tail of the water O-H vibrations with the response of the C-H vibrations of the methyl groups of the oil, they find strong indications that the water molecules at the water/oil interface are preferentially oriented with their hydrogen atoms pointing to the hydrophobic layer. Finally, the Richmond group^{4,18,20} has investigated water/ CCl_4 and water/alkane systems and concluded that the hydrogen bonds between water molecules at these interfaces are significantly weaker than at a water/air interface.

Here we present a VSFG study of the ordering and hydrogen-bonding of water molecules at water/hexane, water/heptane and water/polydimethylsiloxane interfaces. We find evidence that the structure of water at these interfaces is enhanced compared to the structure

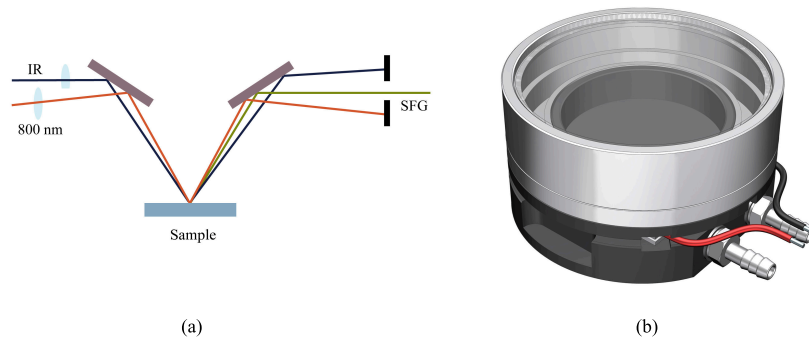


FIG. 2. Schematic illustrations of (a) the intensity SFG setup, (b) the closed cell used for the formation of a hexane or heptane layer on a water surface.

of water at a water/air interface. We also study the structure and hydrogen-bonding as a function of temperature (up to 80°C), because thermodynamic measurements show that hydrophobic interactions are strongly temperature dependent.

II. EXPERIMENTAL

A. SFG setup

The laser source for the VSG setup is a regenerative Ti:Sapphire amplifier producing 800 nm pulses at a 1 kHz repetition rate with a pulse duration of 35 fs and a pulse energy of 3.5 mJ. Approximately one third of the laser output is used to pump a home-built optical parametric amplifier and a difference-frequency mixing stage. This nonlinear optical device produces tunable broad-band mid-IR pulses (range from 2-10 μm , 600 cm^{-1} bandwidth at FWHM, 10-20 μJ). The IR pulses have a sufficiently large bandwidth to measure the complete SFG spectrum of the OH (OD) stretch vibrations of H_2O (D_2O). Another part of the 800 nm pulse is sent through an etalon to narrow down its bandwidth to $\sim 15\text{ cm}^{-1}$. The resulting narrow-band 800 nm pulse (VIS) and the broadband IR pulse are directed to the sample surface at angles of $\sim 50^{\circ}$ and $\sim 55^{\circ}$, respectively, to generate light at the sum frequency. The VIS and IR beams are focused in spatial and temporal overlap on the sample surface with 200 mm and 100 mm focal length lenses, respectively. The SFG light generated at the surface is sent to a monochromator and detected with an Electron-Multiplied Charge Coupled Device (EMCCD, Andor Technologies). All spectra in this paper

were recorded with s-polarised SFG, s-polarised VIS and p-polarised IR (with respect to the plane of incidence). The spectra are normalised to a reference spectrum from z-cut quartz. The frequency resolution of the measured spectra is determined by the bandwidth of the VIS beam and amounts to $\sim 15 \text{ cm}^{-1}$.

B. Materials

The formation of a stable layer of a hydrophobic material on a water surface depends on a subtle balance between short-range and long-range van der Waals forces. For short n-alkanes ($n \geq 4$) complete wetting of the surface is observed, whereas for alkanes with $5 \leq n \leq 8$ incomplete wetting state (partial wetting) occurs, implying a coexistence of an ultrathin layer and lenses on the surface. Alkanes with $n > 8$ form lenses without a thin film¹⁵. The wetting behaviour of alkanes also depends on thermodynamic conditions (temperature or pressure).

In our experiments we form hexane and heptane layers on a water surface by adsorption of the alkanes from their saturated vapors. It was shown with ellipsometry that this technique leads to hexane and heptane layers consisting of a thin film with droplets of micrometer dimensions¹⁵. The formation of alkane layers from saturated vapors was also demonstrated by X-ray reflectometry¹¹. This method of sample preparation strongly reduces the possibility of contamination, because only volatile materials such as alkanes can evaporate and form a layer on water. We used materials like D₂O ($\geq 99.96\%$, Cambridge Isotope Laboratories), n-hexane ($\geq 97.0\%$, Aldrich), heptane ($\geq 99.0\%$, Aldrich), and polydimethylsiloxane (PDMS, $M_r = 162.38$, $\geq 98.5\%$) as received. The water surface was enclosed in a Teflon coated aluminium cell with a CaF₂ window on top, $\sim 2 \text{ cm}$ above the water surface (Fig. 2). The hexane or heptane ($\sim 3 \text{ ml}$) is placed around the water reservoir, and not in contact with the water, after which the cell is sealed. The temperature of the cell can be varied from 0 till 80°C using a peltier element. The top CaF₂ window is heated to $\sim 5^\circ\text{C}$ above the temperature set of the cell, to prevent water condensation. The water/polydimethylsiloxane (PDMS) interface was prepared by depositing $\sim 200 \mu\text{l}$ PDMS directly on the water surface.

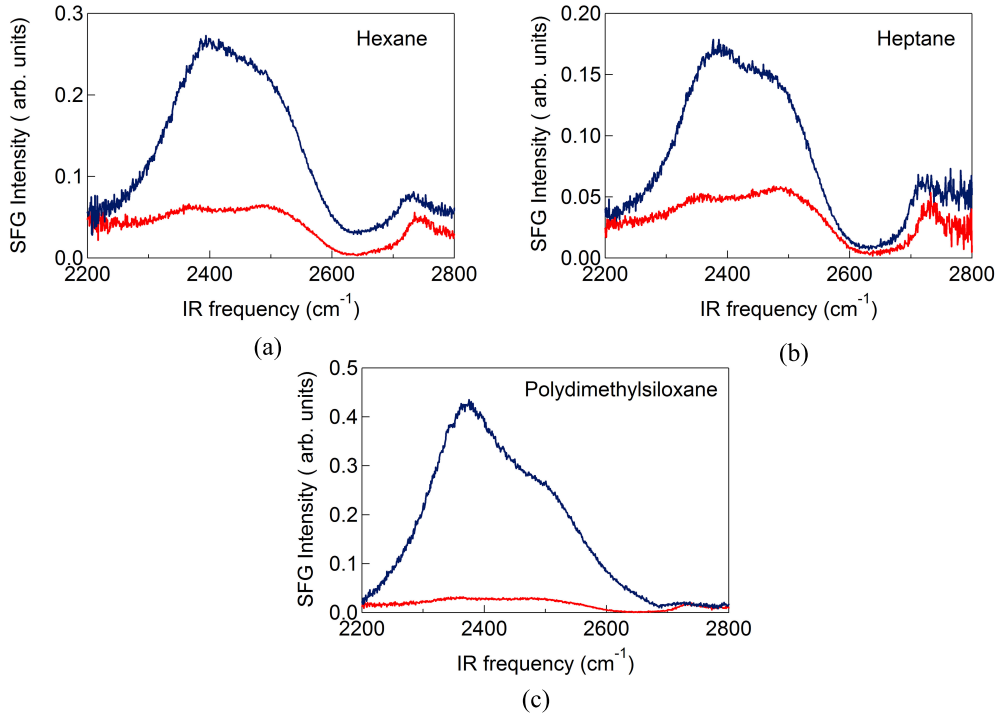


FIG. 3. Intensity SFG spectra of (a) D₂O/air (red) and D₂O/hexane (blue), (b) D₂O/heptane (blue), (c) D₂O/polydimethylsiloxane (blue). All spectra are represented by the blue line and compared with a D₂O/air spectrum (red line).

III. RESULTS

Figure 3 shows intensity SFG spectra in the frequency region of the OD stretch vibrations measured for D₂O/hexane, D₂O/heptane, and D₂O/PDMS. For comparison, we also show the SFG spectrum of a D₂O/air interface (Fig. 3, red line). All spectra have been recorded with a polarisation combination *s*-SFG, *s*-VIS, *p*-IR. With this specific light polarisation combination, water dipoles perpendicular to the surface are probed. The SFG spectrum of the D₂O/air interface shows a broad hydrogen-bonded feature between 2200 - 2600 cm⁻¹ with two distinct peaks (OD(I) at 2360 cm⁻¹ and OD(II) at 2500 cm⁻¹). In addition to this broad feature a sharp peak at 2745 cm⁻¹ is seen, which is associated with the OD stretch vibrations of non-hydrogen bonded OD groups that are sticking out of the surface.

Figure 3 shows that the SFG spectra of the D₂O/hydrophobe interfaces have much higher intensities than the D₂O/air interface. The SFG intensity is proportional to the net ordering of the probed molecular vibrations. Hence, the strong increase in SFG intensity indicates

that there are more water molecules pointing with their dipoles perpendicular to the surface at the D₂O/hydrophobe interfaces. This indicates that water molecules at hydrophobic interfaces are less randomly oriented than at water/air interface. It is also seen in Figure 3 that for the D₂O/hydrophobe interfaces the low-frequency peak (OD(I)) is stronger than the high-frequency peak (OD(II)), whereas for the D₂O/air interface the two peaks are of nearly equal intensity. In a recent study it was shown that these two peaks result from a Fermi resonance of the symmetric OD stretch vibration and the overtone of the bending mode²³. The coupling of the OD stretch and the overtone of the bending vibration leads to a so-called Evans window (region of lower intensity) within the broad band of the symmetric OD stretch vibration, thus giving the appearance of a double-peak structure. The relative intensities of the two peaks around the Evans window are dependent on the average H-bond strength of the water molecules at the interface. In case the hydrogen bonding is enhanced, the low-frequency peak becomes stronger than the high-frequency peak. Hence, the stronger low-frequency peak observed for the D₂O/hydrophobe interfaces indicates that at these interfaces the hydrogen bonds between the water molecules are stronger than at the D₂O/air interface.

Figure 4 presents intensity SFG spectra at different temperatures, up to a temperature of 80°C. For the D₂O/air interface the SFG spectrum does not change dramatically in amplitude. An increase in temperature primarily leads to a decrease of the intensity of the low-frequency part of the hydrogen-bonded spectrum, meaning that the hydrogen bonds between the water molecules become weaker (Fig. 4 (a)). Interestingly, for the water/hydrophobe interfaces the intensity of the SFG spectrum decreases strongly at all frequencies in the hydrogen-bonded region of the spectrum. This observation indicates that the enhanced ordering of water molecules at the hydrophobic interface at room temperature vanishes when the temperature increases (Fig. 4 b - d).

The overall decrease in SFG intensity is accompanied by a relative increase of the high-frequency part of the hydrogen-bonded region of the SFG spectrum relative to the low-frequency part of this spectrum, reflecting a decrease of the average hydrogen-bond strength. For the D₂O/hexane interface the SFG spectrum at 70°C has become similar to that of D₂O/air, because this temperature exceeds the boiling point of hexane (~68°C).

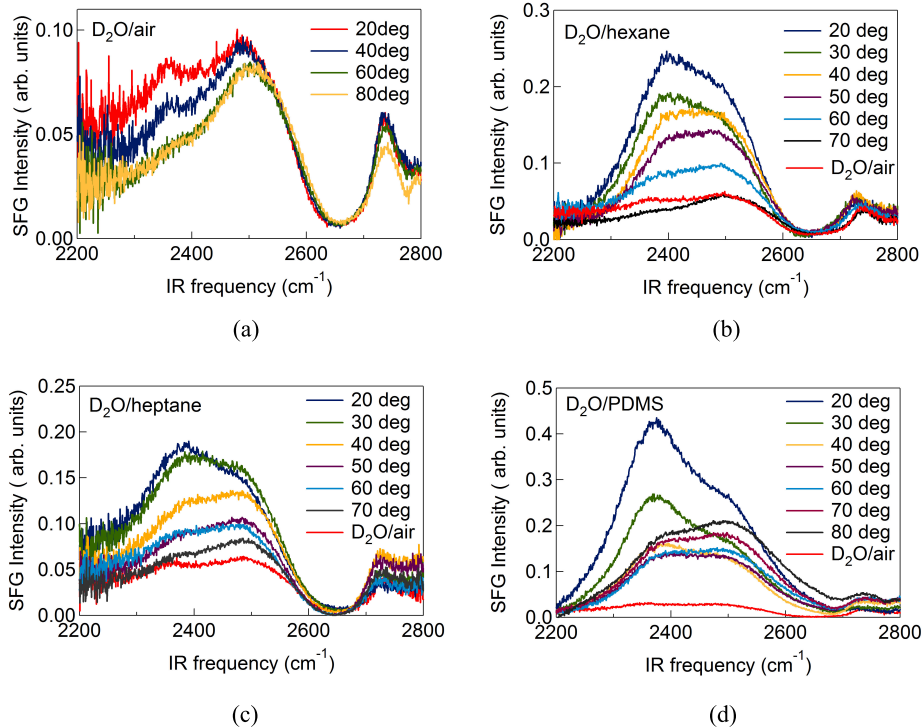


FIG. 4. Intensity SFG spectra of (a) D₂O/air (red), (b) D₂O/hexane (blue), (c) D₂O/heptane (blue), (d) D₂O/polydimethylsiloxane (blue). All spectra are represented by the blue line and compared with a D₂O/air spectrum (red line).

IV. DISCUSSION

We find that at room temperature water shows an enhanced ordering and stronger hydrogen bonding next to a hydrophobic interface. This finding is quite different from the results of previous studies of the intensity SFG spectrum of water/CCl₄ and water/alkane interface^{4,18,20}. In these studies it was found that at room temperature the hydrogen bonding between adjacent water molecules is weaker than at a water/air interface. This difference is probably related to differences in the experimental parameters. The previous work was performed with high-energy (2 mJ at 2.5 μ m to 1 mJ at 4 μ m) nanosecond narrow-bandwidth IR beams²⁰, whereas we use low-energy (\sim 10 μ J) femtosecond broadband IR pulses. Our observation of enhanced order and increased hydrogen bonding of water at hydrophobic interfaces agrees with the results of SFG scattering studies of oil droplets dispersed in water²⁸ and of a Raman spectroscopic investigation of the response of water molecules hydrating

hydrophobic molecular groups in bulk alcohol/water mixtures⁶. Molecular dynamics simulations of water/heptane interface and water/decane interfaces also show the presence of an enhanced ordering of the water molecules at the interface at room temperature^{10,28}.

Theoretical studies showed that the structuring effect of hydrophobes on water strongly depends on the size (radius) of the hydrophobic solute⁵. Small hydrophobic spheres (< 1 nm) fit in well in the hydrogen-bond network and tend to enhance the hydrogen-bond structure. Large hydrophobic spheres are not that well accommodated and in fact give rise to a high concentration of broken hydrogen bonds, thus implying an overall weakening of the hydrogen-bond network. This theoretical description was shown to be extremely successful in describing the thermodynamic properties and aggregation behavior of solutions of hydrophobes. In view of these theoretical findings, it is quite surprising that water would show an enhanced hydrogen-bonded structure at the interface formed by water and a superposed layer of a hydrophobic compound. Naively one would regard the hydrophobic layer as a hydrophobic ball with an infinite radius, from which one would expect the hydrogen-bond network of the nearby water molecules to be disrupted. However, the hydrophobic layer will be highly corrugated on the molecular scale. The interface is therefore likely composed of methyl and methylene groups sticking into the water phase, and their hydration can be viewed as hydrophobic hydration in the small-molecule regime (< 1 nm). This picture agrees with the results of recent molecular dynamics simulations. Knecht et al.¹⁰ showed that there is no enhanced ordering of the water hydrogen-bond network when water is in contact with a smooth hydrophobic wall. The enhanced ordering only arises if the molecular-scale roughness of the hydrophobic interface is accounted for. Of course, the molecular-scale structure of the water/hydrophobic interface is a result of a complex interplay of enthalpy and entropy driving forces of the water and hydrophobic phases, including the interaction between these phases.

We observe that the enhanced ordering of water at room temperature completely vanishes at elevated temperatures. This temperature dependence also agrees very well with the results of the recent Raman spectroscopic study of hydrophobic molecular groups in bulk alcohol/water mixtures⁶. In this latter study it was found that there is even an enhanced disorder at elevated temperatures. The strong temperature dependence of hydrophobic hydration is very much in line with thermodynamic observations and with studies of the dynamics of water hydrating hydrophobic solutes. In femtosecond infrared and NMR spec-

troscopic studies it was found that the reorientation of the water molecules in the hydration shell strongly speeds up when the temperature is increased^{9,14,31}.

An interesting observation is that the temperature dependence of the drop of intensity of the SFG spectrum differs from the temperature dependence of the shape of the spectrum. Up to $\sim 40^\circ\text{C}$ the temperature increase leads to a drop in intensity, while the shape of the spectrum remains rather similar to that at room temperature. At temperatures $>40^\circ\text{C}$ the spectral change is dominated by a blue-shift. This type of behavior is especially clear for the $\text{D}_2\text{O}/\text{PDMS}$ interface for which the hydrophobe concentration will not change when the temperature is increased (in contrast to hexane and heptane that will (partly) evaporate). These findings indicate that the enhanced order of water surrounding hydrophobic molecular groups is even more strongly dependent on temperature than the strength of the average hydrogen-bond interaction. It thus appears that a minor change in temperature already suffices to change the ordering induced by the hydrophobic surface.

V. CONCLUSIONS

We used vibrational sum-frequency generation (VSFG) to study the structure and hydrogen bonding of water at three interfaces with: hexane, heptane and polydimethylsiloxane. For all water/hydrophobe interfaces we observe that the SFG intensity is 4-10 times higher than for a water/air interface. This observation shows that water has a stronger preferential orientation at an interface with a hydrophobic system than at the interface with air. We also observe that the SFG spectrum is red shifted compared to that of a water/air interface, which points at a strengthening of the hydrogen bonds between the water molecules. Together these observations indicate that the water structure is enhanced at the water/hydrophobe interface. With increasing temperature the SFG intensity strongly decreases and the SFG spectrum shows a significant blue-shift, indicating that the ordering of the water decreases. The molecular picture emerging from our studies is that two adjacent layers of water and a hydrophobic system forms a highly corrugated interface with the methyl and methylene groups protruding into the water. These groups then act as a template for the water network to fold around leading to an enhancement of the water structure and the hydrogen-bond interaction.

VI. ACKNOWLEDGMENT

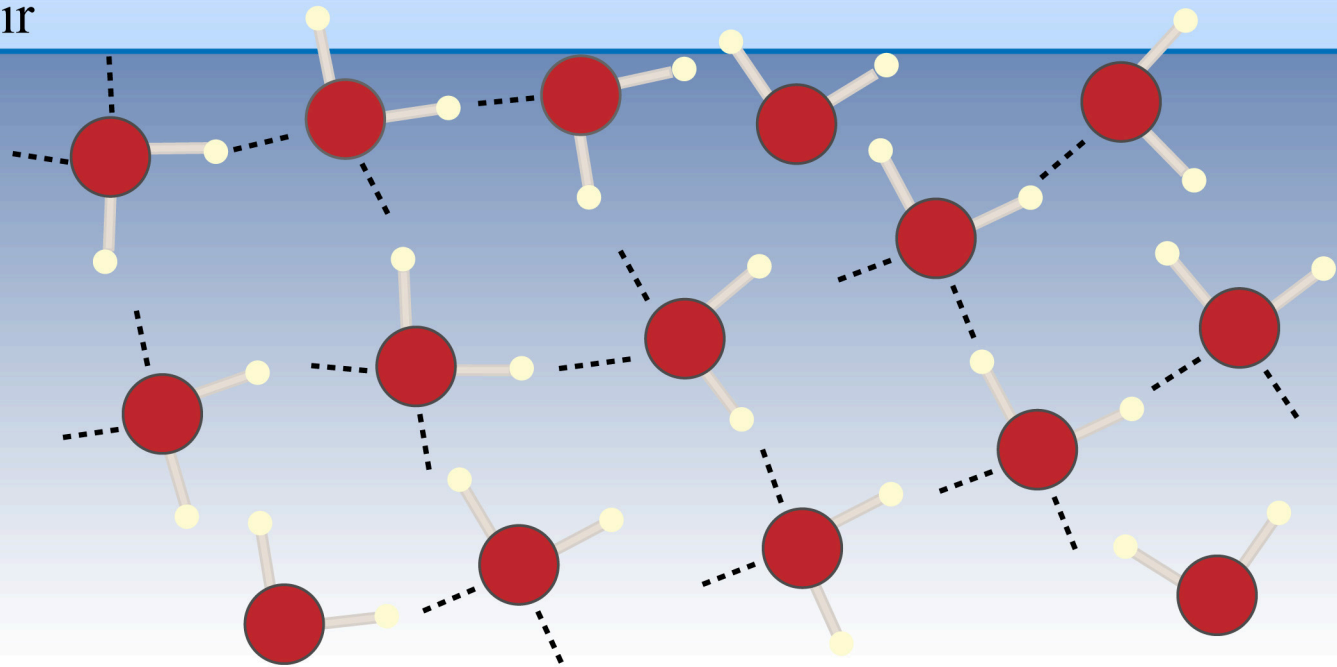
This work is part of the research program of the "Stichting voor Fundamenteel Onderzoek der Materie (FOM)", which is financially supported by the "Nederlandse organisatie voor Wetenschappelijk Onderzoek (NWO)". The work was performed within the framework of a FOM Industrial Partnership Program with Top-institute Wetsus for water research, and is financially supported by Wetsus.

REFERENCES

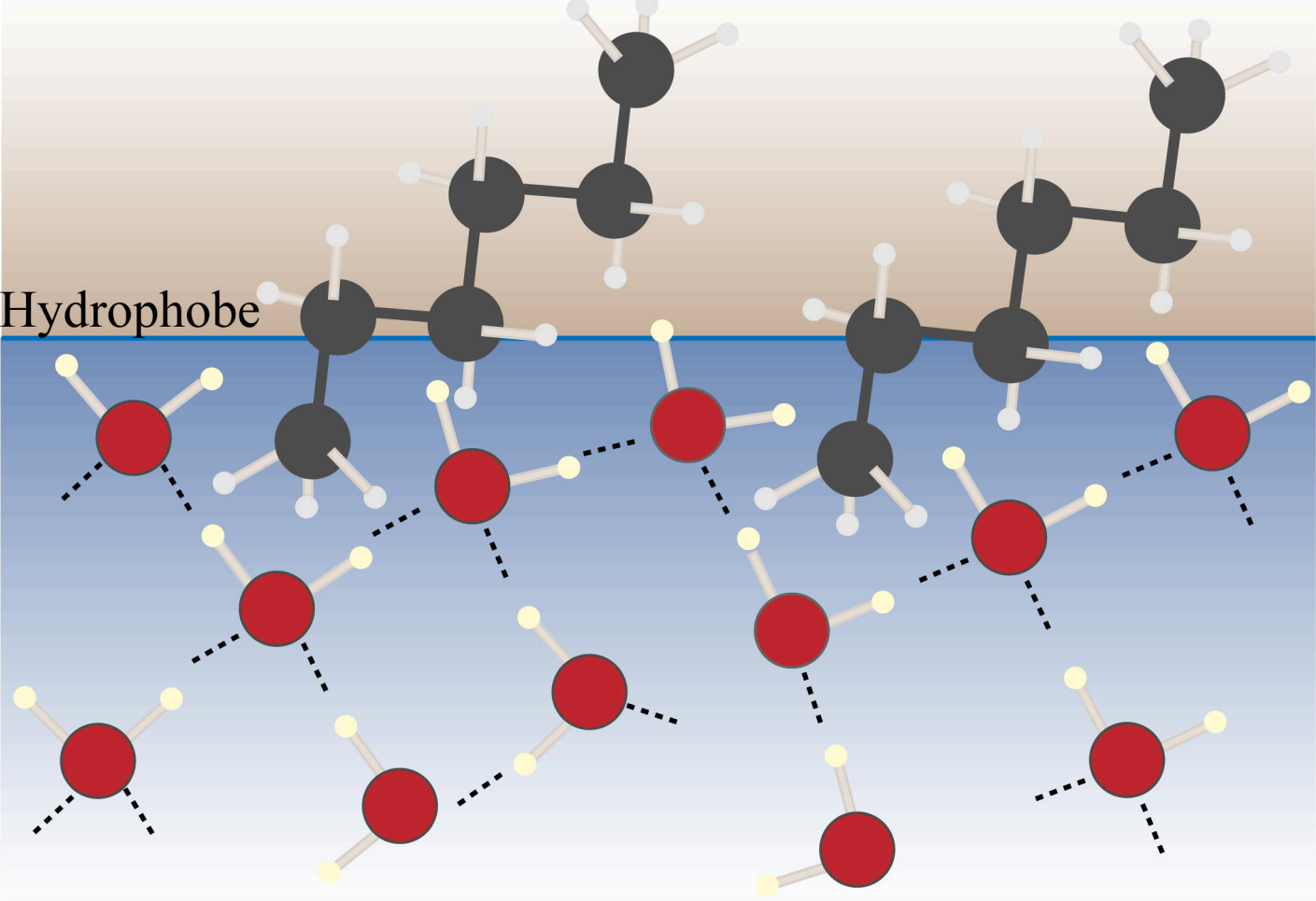
- ¹P. Ball, *Chem. Rev.* **108**, 74-108 (2008).
- ²E. H. G. Backus, J. M. Kuiper, J. B. F. N. Engberts, B.Poolman and Misha Bonn, *J. Phys. Chem.* **115**, 2294-2302 (2011).
- ³A. A. Bakulin, M. S. Pshenichnikov, C. Petersen and H. J. Bakker, *J. Phys. Chem.* **115**, 1821-1829 (2011).
- ⁴M. G. Brown, D. S. Walker, E. A. Raymond and G. L. Richmond, *J. Phys. Chem.* **107**, 237-244 (2003).
- ⁵D. Chandler, *Nature*, **437**, 640-647 (2005).
- ⁶J. G. Davis, K. P. Gierszal, P. Wang and D. Ben-Amotz, *Nature* **491**, 582-585 (2012).
- ⁷S. Dixit, S.J. Crain, W.C.K. Poon, J.L. Finney and A. K. Soper, *Nature* **416**, 829-832 (2002).
- ⁸H. S. Frank and J. W. Evans, *J. Chem. Phys.*, **13**, 507-532 (1945).
- ⁹Y. Ishihara, S. Okouchi and H. Uedaira, *J. Chem. Soc. Faraday Trans.* **93**, 3337-3342 (1997).
- ¹⁰V. Knecht, H.J. Risselada, A.E. Marke and S.J. Marrink, *J. Colloid Interface Sci.* **318**, 477-486 (2008).
- ¹¹O.-S. Kwon, H. Jing, K. Shin, X. Wang and S. K. Satija, *Langmuir* **23**, 12249-12253 (2007)
- ¹²D. Liu, G. Ma, L.M. Levering and H. C. Allen, *J. Phys. Chem* **108**, 2252-2260 (2004).
- ¹³S. Nihonyanagi, S. Yamaguchi and T. Tahara, *JACS* **132**, 6867-6869 (2010).
- ¹⁴C. Petersen, K.-J. Tielrooij and H.J. Bakker, *J. Chem. Phys.* **130**, 2145117 (2009).
- ¹⁵T. Pfohl, H. Mohwald and H. Riegler, *Langmuir* **14**, 5285-5291 (1998).
- ¹⁶E.A. Raymond and G.L.Richmond, *J. Phys. Chem.* **108**, 5051-5059 (2004).

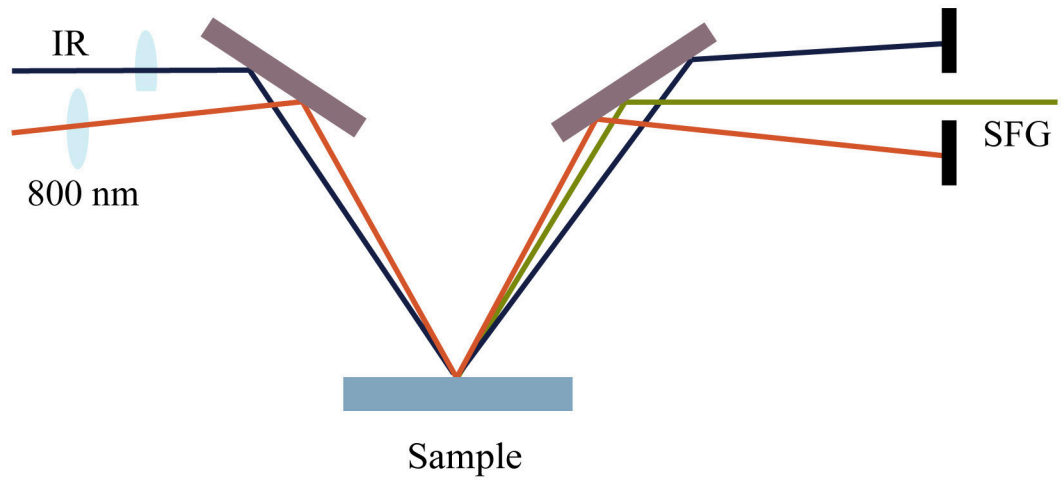
- ¹⁷Y. L. A. Rezus and H. J. Bakker, *Phys. Rev. Lett.* **99**, 148301 (2007).
- ¹⁸L. F. Scatena, M. G. Brown and G. L. Richmond, *Science* **292**, 908-912 (2001).
- ¹⁹L. F. Scatena and G. L. Richmond, *Chem. Phys. Lett.* **383**, 491-495 (2004).
- ²⁰L. F. Scatena and G. L. Richmond, *J. Phys. Chem.* **105**, 11240-11250 (2001).
- ²¹P. C. Singh, S. Nihonyanagi, S. Yamaguchi and Tahei Tahara, *J. Chem. Phys.* **137**, 094706 (2012).
- ²²A.K. Soper and J.L. Finney, *Phys. Rev. Lett.* **71**, 4346-4349 (1993).
- ²³M. Sovago, R. K. Campen, G. W. H. Wurpel, M. Muller, H. J. Bakker and M. Bonn, *Phys. Rev. Lett.* **100**, 173901 (2008).
- ²⁴M. Sovago, G. W. H. Wurpel, M. Smits, M. Muller and M. Bonn, *J. Am. Chem. Soc.* **129**, 11079 (2007).
- ²⁵C. Tian, S. J. Byrnes, H.-L. Han and Y. R. Shen, *J. Phys. Chem. Lett.* **2**, 1946-1949 (2011).
- ²⁶C. S. Tian and Y. R. Shen, *PNAS* **106**, 15148-15153 (2009).
- ²⁷J. T. Titantah and M. Karttunen, *J. Am. Chem. Soc.* **134**, 9362-9368 (2012).
- ²⁸R. Vacha, S. W. Rick, P. Jungwirth, A. G. F. de Beer, H. B. de Aguiar, J.-S. Samson and S. Roke, *J. Am. Chem. Soc.* **133**, 10201-10210 (2011).
- ²⁹W.Hua, A.M. Jubb and H. C. Allen, *J. Phys. Chem.* **2**, 2515-2520 (2011).
- ³⁰S. Ye, S. Nihonyanagi and K. Uosaki, *Phys. Chem. Chem. Phys.* **3**, 3463-3469 (2001).
- ³¹K. Yoshida, K. Ibuki and M. Ueno, *J. Chem. Phys.* **108**, 1360-1367 (1998).
- ³²S. Roke, J. Schins, M. Muller and M. Bonn, *Phys. Rev. Lett.* **90**, 128101 (2003).
- ³³D. Laage, G. Stirnemann and J.T. Hynes, *J. Phys. Chem.* **113**, 2428-2435 (2009).

Air



Hydrophobe

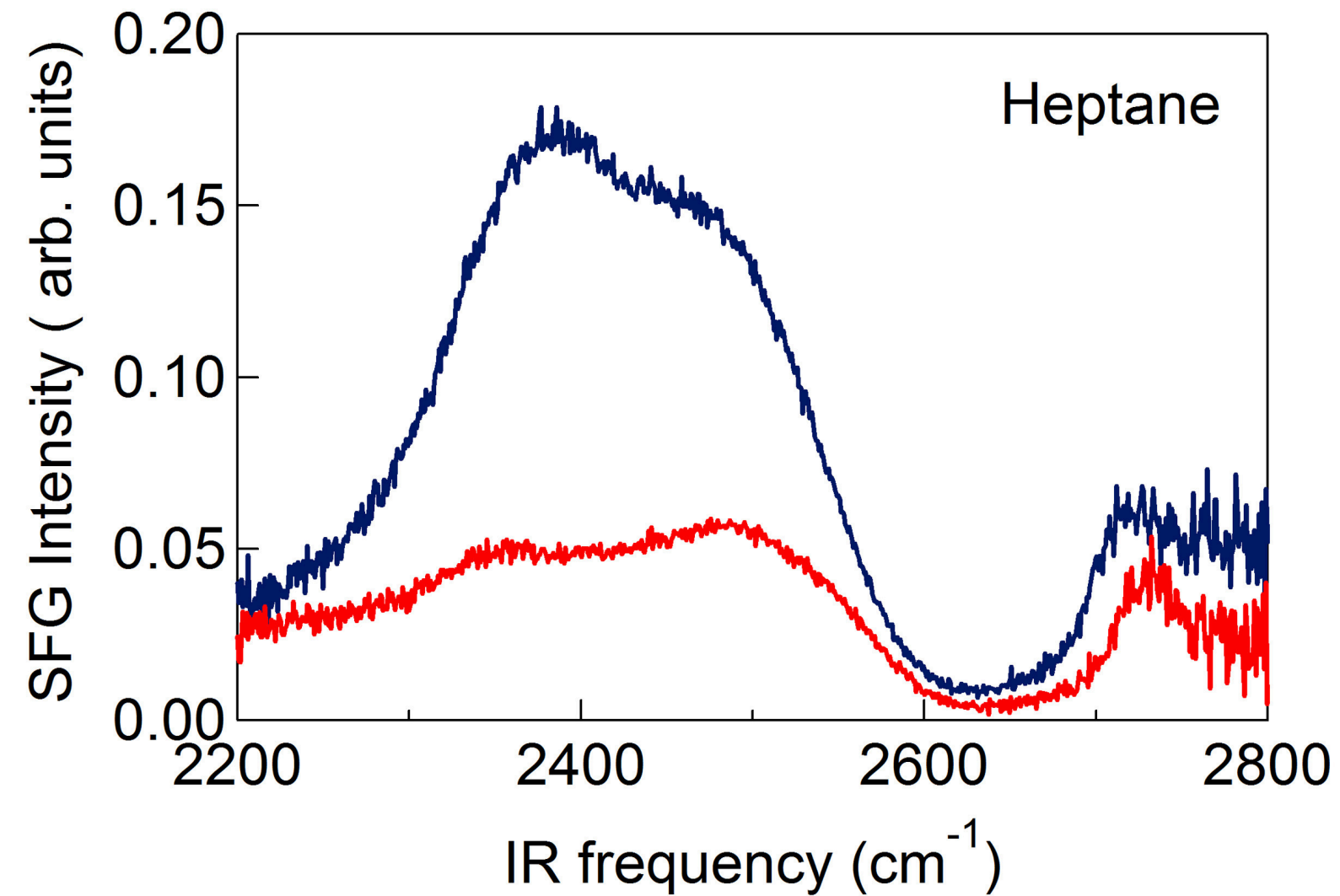
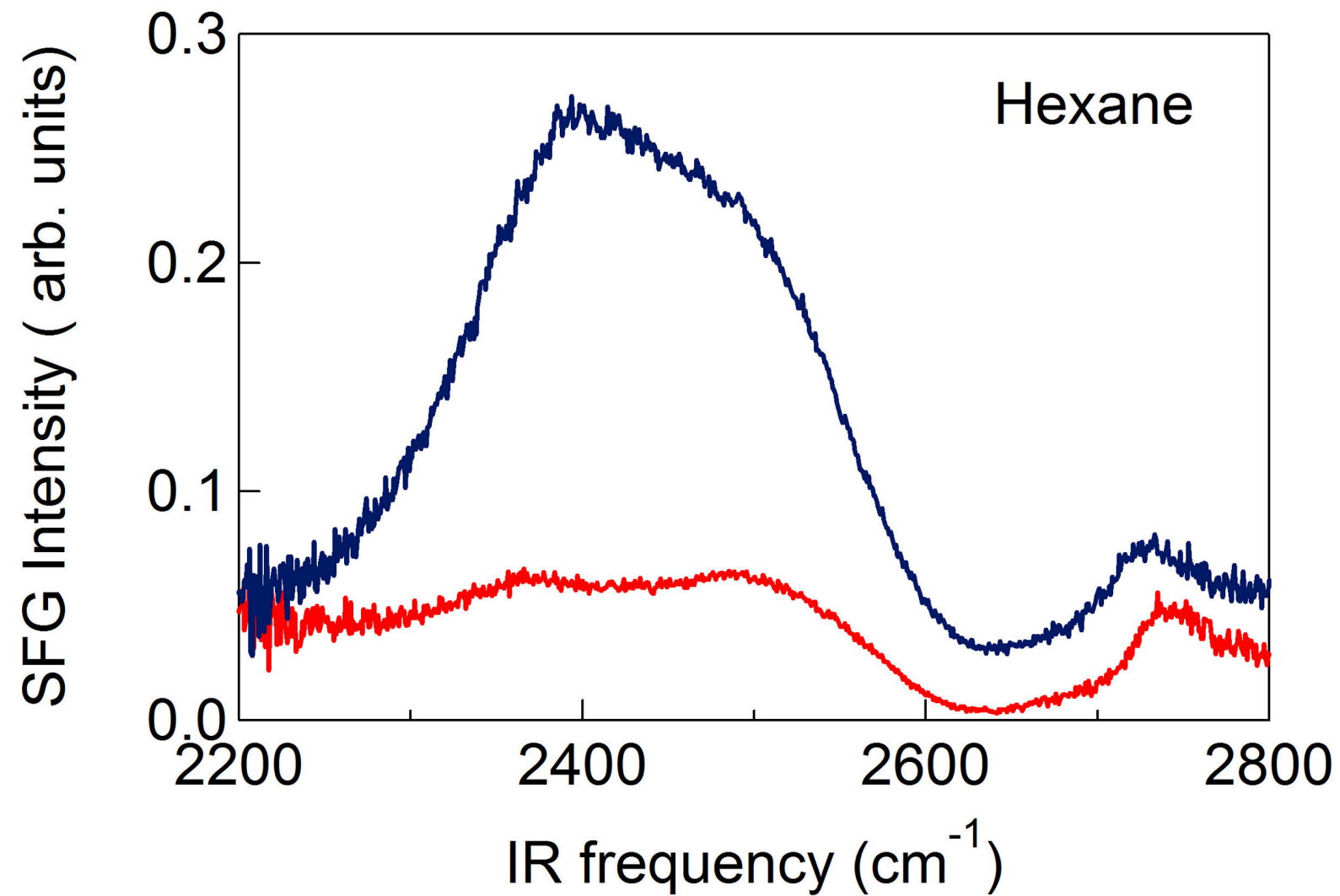




(a)

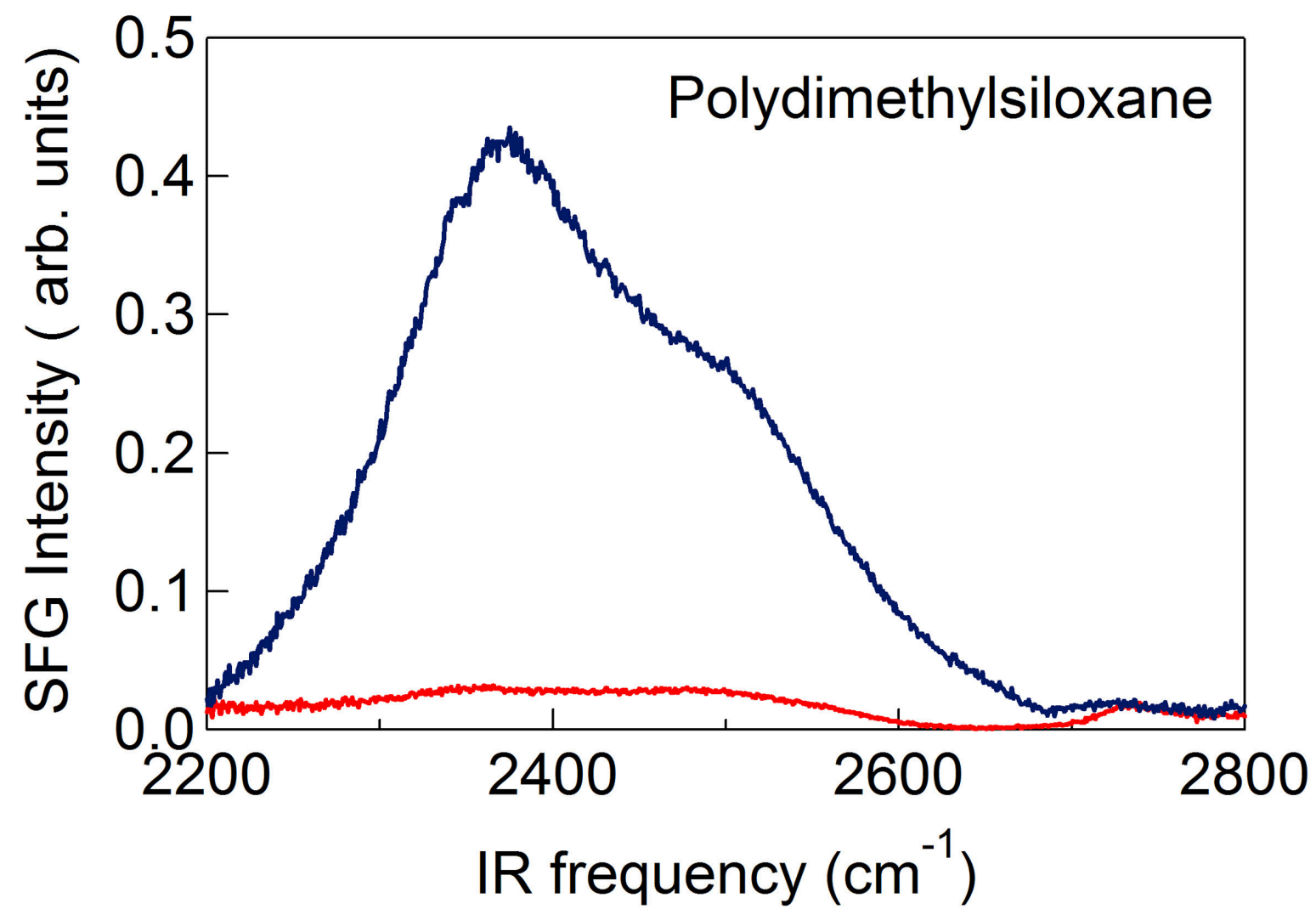


(b)

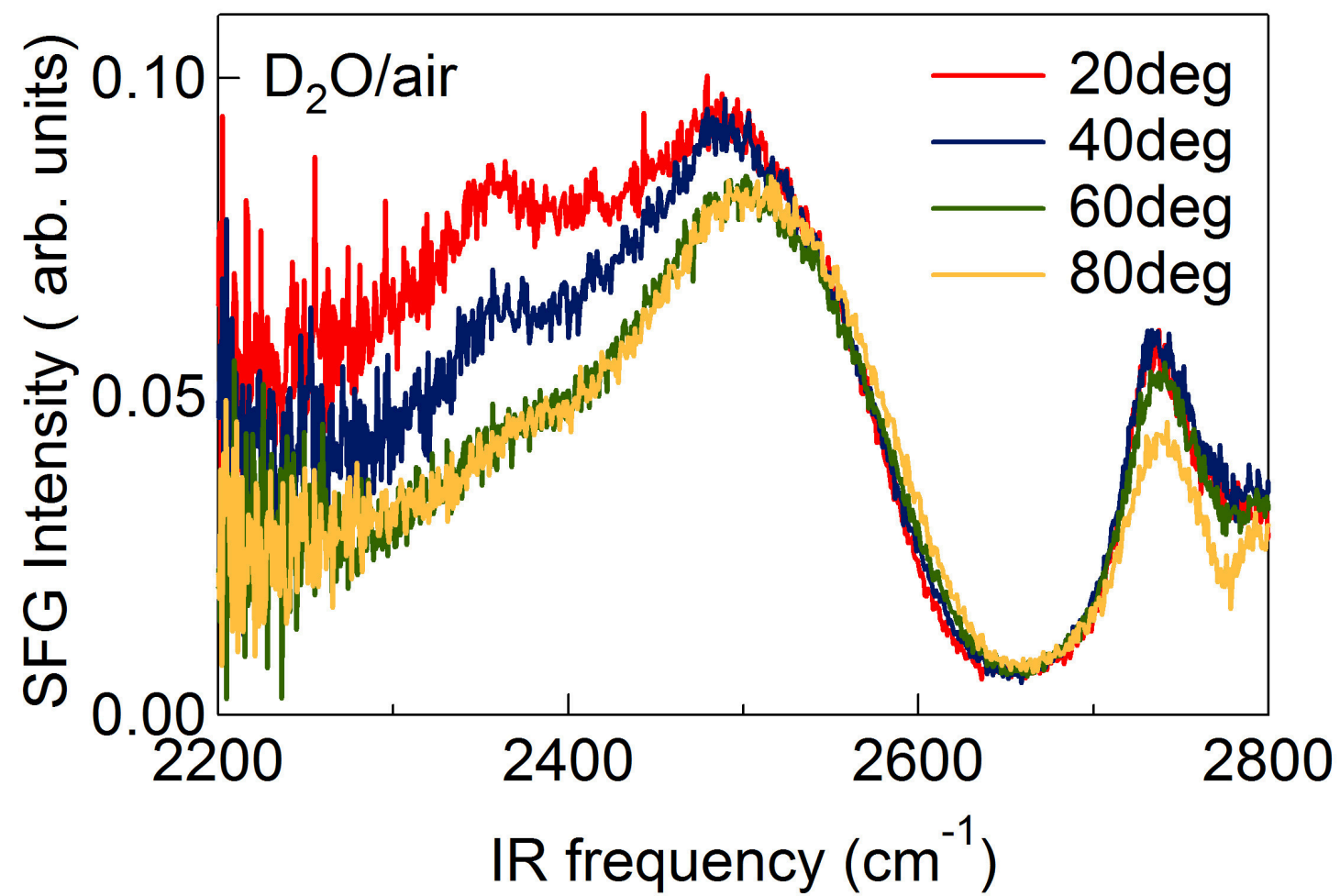


(a)

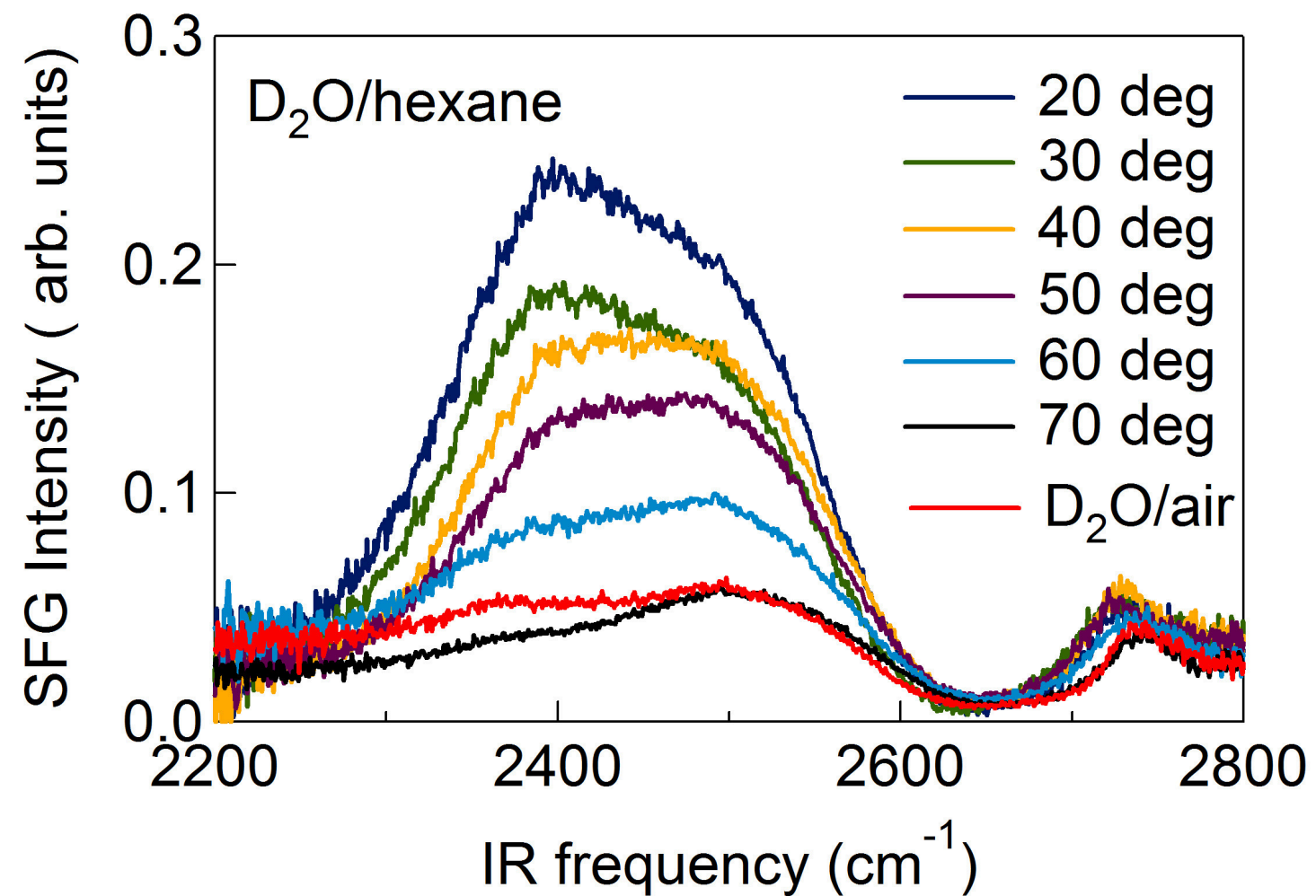
(b)



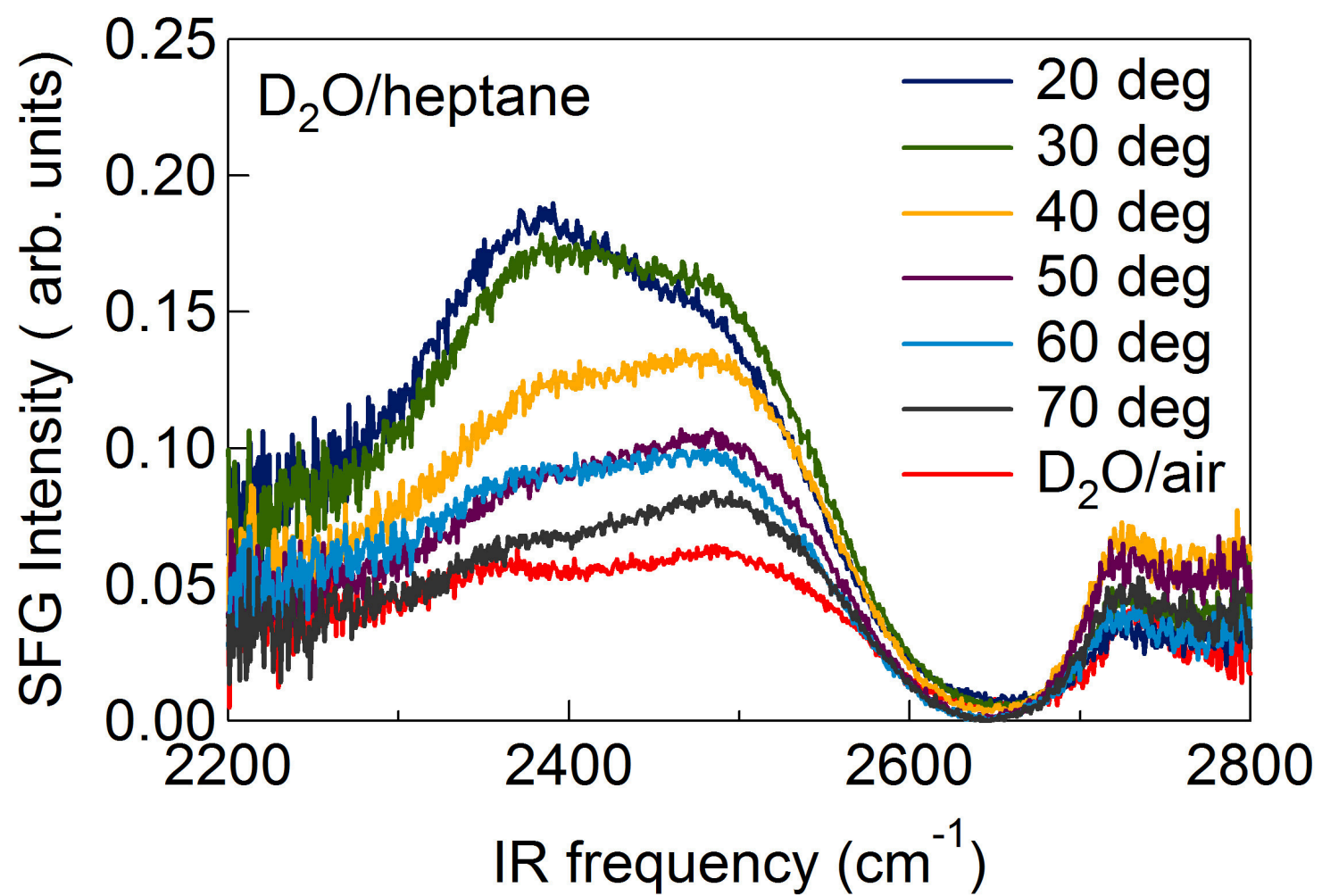
(c)



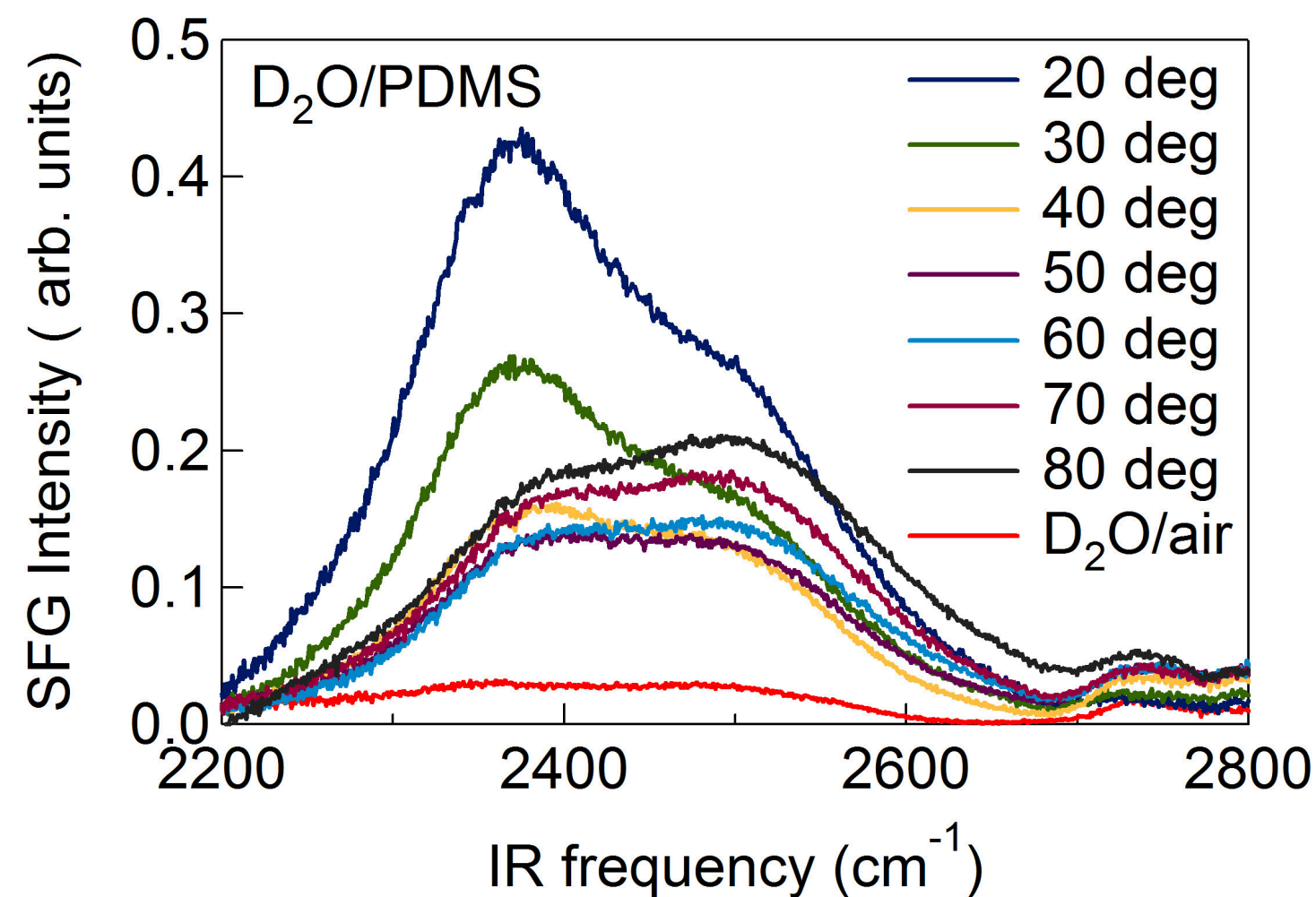
(a)



(b)



(c)



(d)